

Focusing Radially Polarized Light by a Concentrically Corrugated Silver Film without a Hole

Piotr Wróbel,* Jacek Pniewski, Tomasz J. Antosiewicz, and Tomasz Szoplik

Faculty of Physics, University of Warsaw, Pasteura 7, 02-093 Warsaw, Poland

(Received 15 December 2008; revised manuscript received 9 April 2009; published 8 May 2009)

We report a phenomenon of focusing a radially polarized beam from the visible range by a silver film with no hole on the optical axis and double-sided concentric corrugations. The axes of symmetry of grooves and the illuminating beam coincide. An Ag lens of 100 nm thickness, five grooves, of which the outermost has 5 μm diameter, at $\lambda = 400$ nm transmits 22% of electric energy and focuses light into a $0.2\lambda^2$ spot area at a focal length close to 2λ , while at $\lambda = 500$ nm the results are 11%, $0.16\lambda^2$ and λ , respectively. This Ag lens focuses without contribution of evanescent waves a far-field source into a far-field spot. The nanolens acts like a refractive optical system of high numerical aperture close to unity.

DOI: 10.1103/PhysRevLett.102.183902

PACS numbers: 41.20.Jb, 42.79.-e

Interest in enhanced transmission of light through sub-wavelength holes in metal nanolayers originates from a seminal paper of Ebbesen *et al.* [1]. Enhancement means that the amount of transmitted light related to that of impinging onto the holes exceeds unity. The intensity of transmitted light increases even more when a single aperture of diameter $a \ll \lambda$ is surrounded by a set of concentric, periodic, and subwavelength corrugations which permit excitation of surface plasmon-polaritons (SPPs) [2]. Precise control of periodicity, shape, and depth of grooves milled in the metal film surface on one or both sides leads to controlled divergence of transmitted beams [3–5]. Beaming light is observed in near and far fields of diffraction and depends on angle of incidence and polarization of light [3]. For a case of linearly polarized light with E field perpendicular to grooves of a grating, the effect of beaming is explained in terms of surface plasmon resonances which couple to radiative modes behind the metal film [4].

A step forward in studies on enhanced transmission through a nanohole surrounded by periodic corrugations was made when focusing properties of a single subwavelength slit flanked symmetrically by equally spaced grooves were theoretically predicted in [6] and experimentally confirmed in [7]. It was shown that focusing of linearly polarized incident light is possible when E field components perpendicular to grooves, due to a proper choice of resonance cavity parameters, are maximum in subsequent indentations and interfere constructively. The parameters in question are the aperture diameter and groove width a , groove lattice constant Λ , and groove depth h . Moreover, the resonance wavelength-to-lattice constant λ/Λ ratio depends only on the number of grooves N . For p -polarized plane wave illumination with $\lambda = 532$ nm, $\Lambda = 500$ nm, $a = 40$ nm, and $h = 83.5$ nm the calculations gave a 30 μm long focal region with the maximum concentration of energy distant 46.3 μm from the metal film back surface [6]. Such long and wide focal regions are characteristic for axicons, where conical waves diffracted with a single spatial frequency on subsequent structure elements focus in subsequent planes along the

propagation axis. Surface plasmon optics was recently summarized [8] and potential applications in nano-optics, microscopy, and plasmonic circuitry were described. In connection with these possibilities, the present authors proposed to improve resolution of tapered-fiber metal-coated aperture probes for scanning near-field optical microscopy (SNOM) due to enhanced energy throughput [9]. Corrugations of dielectric-metal interface improve efficiency of photon-to-plasmon momentum matching and allow for decrease of probe aperture diameter.

Transmission of light through continuous and corrugated metal films has been analyzed by several authors [10–18]. Weber and Mills [10] considered cross coupling of SPPs in a silver layer of 30 nm on a shallow dielectric grating. Because of the constant thickness of the film the cross coupling between surface plasmon modes was weak; however, for a film thin enough of the surface polaritons radiated on both sides of the film. Inagaki *et al.* [11] experimentally confirmed the existence of coupled SPP modes on Ag films of thicknesses from 26 to 121 nm with shallow periodic corrugations. It was shown that a plasmon generated on the front textured metal surface couples efficiently to the back surface when the thickness of the metal film is varied over the corrugation period [12]. Bonod *et al.* [14] reported 80% transmission in the spectral vicinity of plasmon resonance through a continuous 70 nm thin Ag film with sinusoidal grooves. Transmission through metal films without holes depends on the periodicity and shape of grooves and can exceed the transmission of a flat film of the same effective metal thickness by more than 2 orders of magnitude at the wavelengths of surface plasmon Bloch modes [16], as was experimentally verified [17]. Steele *et al.* [18] observed that SPP focusing on circular gratings is maximized when interference between symmetric and asymmetric plasmon modes is avoided.

In this Letter we propose a nanolens in the form of a silver nanolayer with concentric corrugations on both surfaces and no hole at the optical axis. It focuses a radially polarized Laguerre-Gauss (LG) beam of wavelengths from the visible range into spots of full width at half maximum

equal to about 0.46λ . At $\lambda = 500$ nm this plasmonic lens has a focal length equal to λ and acts as a high-NA refractive optical system of $\text{NA} = 0.98$. At $\lambda = 400$ nm the focal length is 2λ and $\text{NA} = 0.92$.

For Drude model dispersion the wavelengths of plasmons on the Ag/air interface are $\lambda_{\text{SPP}} = 210$ and 310 nm when light wavelengths in vacuum are 400 and 500 nm, respectively.

When linearly polarized light illuminates a slit with periodic corrugations on both sides, which are perpendicularly oriented with respect to E field, the photon-to-plasmon coupling is not 100% efficient, even if reflection is neglected. This is because light beams of finite spatial extent have different directions of linear polarization at different points of space [19]. Thus, only part of the beam energy is coupled to plasmons and reradiated with preserved polarization. The rest partially transmits through the thin film, reradiates and blurs the focus decreasing the signal-to-noise ratio in the focal region. Circular concentric grooves that collect linearly polarized light destroy polarization because distribution of charge density ρ_p generated on subsequent p grooves of the metal grating is

$$\rho_p(r, \phi) \propto \cos(N\phi) \cos(\omega t) \delta(r - R_p), \quad (1)$$

where N is the number of quasipoles induced on grooves and R_p are radii of subsequent grooves [20]. In metallic or metal-coated SNOM tips an improvement of photon-plasmon coupling was achieved due to radially polarized LG beams impinging onto smooth or corrugated surfaces [21,22]. LG beams with rotational symmetry of the electric-field distribution that is pure radial or azimuthal polarizations are known for their low-loss propagation in waveguides and nondiffractive behavior in free space. Moreover, a radially polarized beam may be focused with high-NA optics into a sharper focal spot than linearly or azimuthally polarized ones [23,24]. Beams with radial polarization are generated directly in laser resonators on c -cut birefringent Nd: YVO₄ crystals in infrared [25]. In the visible range, they are synthesized in interferometers either from left- and right-handed circularly polarized doughnut modes [26] or from a linearly polarized beam modified using a sectioned half-wave plate [27].

In a computer experiment we analyze a phenomenon of focusing radially polarized light with an unperforated silver thin film with double-sided concentric nanocorrugations. Simulations are performed in cylindrical coordinates with the finite difference time domain (FDTD) method using freeware package Meep [28] and in-house body-of-revolution FDTD code. As shown in Fig. 1, we consider a silver nanolayer of thickness $d = 100$ nm with an on-axis stop of diameter 800 nm, and a set of five concentric grooves of lattice constant $\Lambda = 500$ nm. Groove depth is $h = 40$ nm and width $w = 100$ nm. The axis of symmetry of corrugations coincides with the optical axis of the incident LG beam with pure radial polarization and radial beam profile

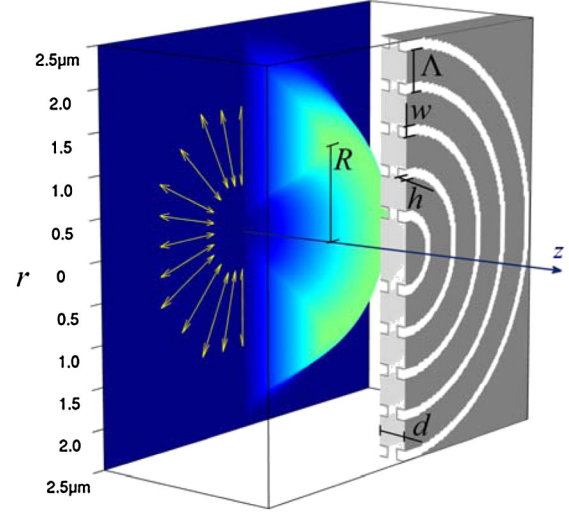


FIG. 1 (color online). Light beam with Laguerre-Gauss intensity profile and pure radial polarization indicated by yellow arrows illuminates an apertureless silver film of a thickness $d = 100$ nm along the z axis. The depth and the width of periodic corrugations with lattice constant $\Lambda = 500$ nm are equal $h = 40$ nm and $w = 100$ nm, respectively. The radius of the maximum intensity of the beam is R .

$$E_r^I(r) = (r/R) \exp(-r^2/2R^2), \quad (2)$$

where radii of maximum intensity $R = 1400$ and 2500 nm.

The plot in Fig. 2(a) shows a doughnut shape of amplitude of the incident electric field radial component E_r^I (solid line) of the beam which is cylindrically symmetric in both intensity and polarization. In the radiated beam the amplitude of radial component E_r^T (dashed line) is calculated 2 nm behind the lens. A qualitatively similar plot of transmitted E_z^T is presented in Fig. 2(b), where the amplitude of the radiated longitudinal component is larger than that of the incident beam. Note, that the plots of Fig. 2 show radial amplitude profiles, thus to assess energy transmitted through subsequent double-sided grooves one must integrate along their circumferences.

The focusing effect can be commented from the diffractive optics point of view. It was proved in terms of vector diffraction theory that the tightest focal spot achievable with high-NA optics is possible when the amplitude of a radially polarized beam increases monotonically with distance to the optical axis within the aperture clearance, what leads to a strong boundary diffraction wave [29]. The highest spatial frequencies, generated at the aperture edge, have the highest amplitude and sharpen the focus. In our case the effective lens clearance is filled with grooves and we illuminate as many of them as possible with high amplitude radial component of electric field. When radius R changes from 1400 to 2500 nm, the increasing part of the energy goes beyond the grooves and transmission decreases. Distributions presented in Fig. 2 can also be commented from the plasmon-polariton point of view which comprises the rest of the Letter.

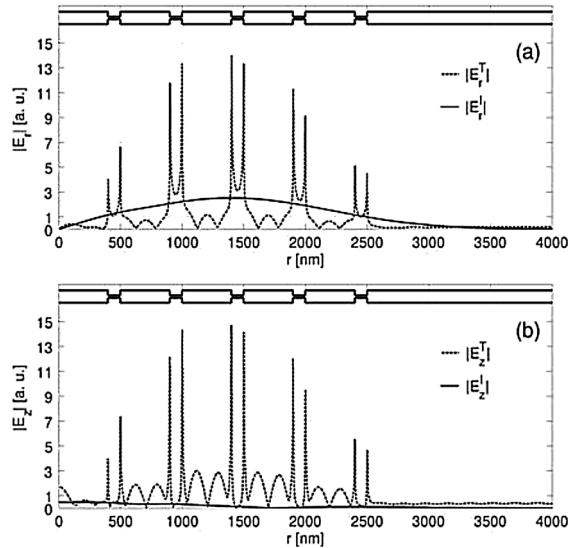


FIG. 2. Distributions (a) of the radial component of the incident electric field amplitude E_r^I at the front plane of the lens (solid) and transmitted E_r^T 2 nm behind the back side (dashed); (b) of the longitudinal component of the incident electric field amplitude E_z^I at the front plane of the lens (solid) and transmitted E_z^T 2 nm behind the back side (dashed). Plots are calculated for $\lambda = 410$ nm and $R = 1400$ nm.

Figure 3 shows spectral intensity transmission, reflection, and absorption characteristics of the nanolens and four distinct spectral ranges (SR) are indicated. In Fig. 4 distributions of electric energy density of total electric field $|E|^2$ for four wavelengths representative for the SRs are presented. SR1 wavelengths from 385 to 445 nm are collimated into λ long focal regions which begin about 500 nm from the lens, have focal lengths of about 2λ . With increase of wavelengths within SR1 the focal region approaches the lens and polaritons become more pronounced. In SR1, transmission is locally enhanced while losses and reflection are simultaneously reduced. In SR1 light transfer results from plasmon modes resonant on both sides of the nanolens [Fig. 4(a)] which are generated due to the groove periodicity $\Lambda - w = 2\lambda_{\text{SPP}}$. Distribution of plasmons corresponds to that of radial component of the incident elec-

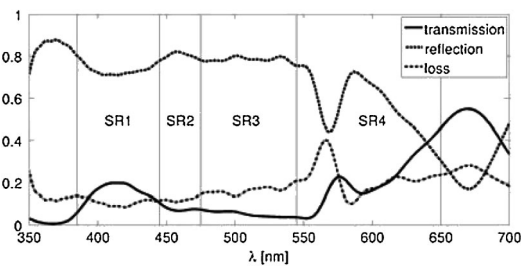


FIG. 3. Plots of transmission, reflection, and absorption of the nanolens. Out of four spectral ranges with different beam shaping properties: SR1 = 385–445 nm; SR2 = 445–475 nm, SR3 = 475–545 nm, and SR4 = 545–650 nm, focusing is observed in SR1 and SR3 only.

tric field and does not show a radial shift. We interpret the light transmission mechanism in SR1 as resonant tunneling between standing SPPs localized on the whole lens and enhanced on groove ridges on both sides [Fig. 4(a)]. This is in accordance with previous studies on thin Ag films with spatially coinciding v-shaped [13] and laterally shifted rectangular [15] grooves. In SR2 (445–475 nm) there is no focusing and light is concentrated in the near-field only [Fig. 4(b)]. In SR3 (475–545 nm) both focal lengths and focal regions are shorter than in SR1 what is similar to refractive lenses where shorter focal length is connected with smaller FWHM and shorter focal region [Fig. 4(c)]. In this range transmission is below 10%, meaning that the structure is out of SPP resonance. At the back circularly grooved surface of the lens, interference of generated plasmon eigenmodes redistributes electric energy density toward the axis [Fig. 4(c)]. For $\lambda = 500$ nm decrease of groove depth from 40 to 10 nm limits the number of generated eigenmodes to higher orders what results in a reduction of intensity transmission by a factor of 20 and a gradual increase of focal length by 100 nm. For the thickest span focusing eventually ceases. In SR4 (545–650 nm) high transmission and no focusing are observed [Fig. 4(d)]. In Fig. 4(b) and 4(d) plasmons on the lens back side propagate radially toward the system axis and constructively interfere at the on-axis stop, limiting the aperture and destroying focusing. A similar distribution of plasmons on circular gratings was observed in SNOM measurements by Steele *et al.* [18].

Within SR1 and SR3 the full width at half maximum (FWHM) of beams in focus are equal to about 0.46λ , which is similar to focal widths achievable with high-NA refractive optical systems and radially polarized illumination [22,23]. NA describes the range of angles over which the system emits light and for high-NA objectives have a narrow point spread function. Thus, the unperforated silver thin film with concentric double-sided nanocorrugations acts as a high-NA lens.

The FWHM and length of the focal region, smaller than for axicons, clearly shows that the focusing phenomenon

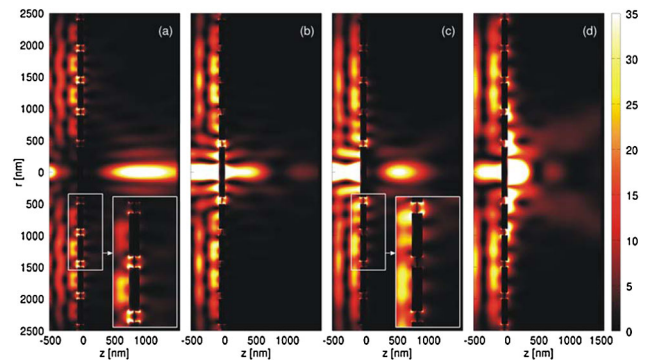


FIG. 4 (color online). Normalized electric energy density $|E|^2$ distribution in the vicinity of the nanolens for $R = 1400$ nm for wavelengths (a) 410 nm, (b) 460 nm, (c) 500 nm, and (d) 600 nm.

cannot be explained solely in terms of SPP resonances on a five-groove circular structure, which is much different from an ordinary 1D grating. Another mechanism of light transmission into far field is connected with plasmon eigenmodes in double-sided grooves of a cylindrically symmetric grating. The role of plasmon eigenmodes was discussed earlier for metal cylinders with a dielectric core [30] and thin metallic films with various 1D surface profiles [18,31,32]. A detailed analysis of plasmon eigenmodes of grooves as a function of their width, depth, and periodicity and interference of SPPs launched by grooves is beyond the scope of this Letter.

Focusing of radially polarized light into a tight spot results from two independent factors. The first is highly efficient photon-to-plasmon coupling which is possible due to almost 100% radial polarization achievable also in experiment [27]. Thus, the amount of light with linear or azimuthal polarization is negligible and there is virtually no background emission that decreases the signal-to-noise ratio in the focal region.

The second is connected with evolution of radial and longitudinal components of transmitted electric field behind the lens. Ridge enhanced maxima of the radial E_r^T and longitudinal E_z^T components of emitted electric field are shown in Fig. 2. The field E_r^T on subsequent corrugations is in phase and propagates as higher order radially polarized beams. The longitudinal components E_z^T influence convergence of transmitted beam. In both ranges SR1 and SR3 the radial and longitudinal components have comparable amplitudes along the radius, but in SR3 light is concentrated near the axis. The radial components of E_r^T interfere destructively on the axis. Light emitted from oscillating electrons propagates in such a way that the longitudinal component of electric field E_z^T is especially reinforced due to constructive interference. In the focal region the energy is transferred from the radially polarized electric field components to longitudinally polarized ones and the longitudinal component of electric field E_z^T is about 10 times stronger than E_r^T incident onto the structure. Reinforcement of the axial component E_z^T depends on the number of illuminated grooves and range of plasmons.

In conclusion, we have presented a 3D silver nanolens with concentric corrugations on both surfaces and no hole on the optical axis. The nanolens, when illuminated with a radially polarized visible range Laguerre-Gauss beam focuses light into spots of FWHM equal 0.46λ . Focal lengths depend on wavelength and range from one to a few λ . Because of constructive interference of far-field radiation of SPPs generated on the back side the lens focuses without contribution of the evanescent field. There are two aspects of the mechanism governing scattering of light on the back side of the lens. In the first, SPPs resonant with illumination from the range of wavelengths from 385 to 445 nm couple on the opposite interfaces without radial redistribution. In the second, SPPs not resonant with incident light ($\lambda = 475\text{--}545$ nm) couple to the back side and radially

redistribute closer to the axis. The proposed nanolens concentrates radially polarized LG illumination as tightly as classical high-NA refractive optical systems.

This research was sponsored by the Polish Ministry of Science and Higher Education Grant No. N N507 445534 and No. 0694/H03/2007/32. The authors are partners in COST Actions MP 0702 and MP 0803. Numerical computations were performed in the ICM, University of Warsaw, Grant No. G33-7.

*Corresponding author.

piotr.wrobel@igf.fuw.edu.pl

- [1] T. W. Ebbesen *et al.*, Nature (London) **391**, 667 (1998).
- [2] T. Thio *et al.*, Opt. Lett. **26**, 1972 (2001).
- [3] H. J. Lezec *et al.*, Science **297**, 820 (2002).
- [4] L. Martin-Moreno *et al.*, Phys. Rev. Lett. **90**, 167401 (2003).
- [5] F. I. Baida, D. Van Labeke, and B. Guizal, Appl. Opt. **42**, 6811 (2003).
- [6] F. J. Garcia-Vidal *et al.*, Appl. Phys. Lett. **83**, 4500 (2003).
- [7] L. Verslegers *et al.*, Nano Lett. **9**, 235 (2009).
- [8] W. L. Barnes, A. Dereux, and T. W. Ebbesen, Nature (London) **424**, 824 (2003).
- [9] T. J. Antosiewicz and T. Szoplik, Opt. Express **15**, 10920 (2007).
- [10] M. G. Weber and D. L. Mills, Phys. Rev. B **32**, 5057 (1985).
- [11] T. Inagaki *et al.*, Phys. Rev. B **32**, 6238 (1985).
- [12] U. Schröter and D. Heitmann, Phys. Rev. B **60**, 4992 (1999).
- [13] W. C. Tan, T. W. Preist, and R. J. Sambles, Phys. Rev. B **62**, 11134 (2000).
- [14] N. Bonod *et al.*, Opt. Express **11**, 482 (2003).
- [15] D. Gérard *et al.*, Phys. Rev. B **69**, 113405 (2004).
- [16] D. Gérard *et al.*, Opt. Express **12**, 3652 (2004).
- [17] B. Bai, L. Li, and L. Zeng, Opt. Lett. **30**, 2360 (2005).
- [18] J. M. Steele *et al.*, Opt. Express **14**, 5664 (2006).
- [19] J. Lekner, J. Opt. A Pure Appl. Opt. **5**, 6 (2003).
- [20] T. J. Antosiewicz and T. Szoplik, Opt. Express **15**, 7845 (2007).
- [21] N. A. Janunts *et al.*, Opt. Commun. **253**, 118 (2005).
- [22] F. I. Baida and A. Belkhir, Plasmonics **4**, 51 (2009).
- [23] S. Quabis *et al.*, Opt. Commun. **179**, 1 (2000).
- [24] K. S. Youngworth and T. G. Brown, Opt. Express **7**, 77 (2000).
- [25] K. Yonezawa, Y. Kozawa, and S. Sato, Opt. Lett. **31**, 2151 (2006).
- [26] S. C. Tidwell, D. H. Ford, and W. D. Kimura, Appl. Opt. **29**, 2234 (1990).
- [27] S. Quabis, R. Dorn, and G. Leuchs, Appl. Phys. B **81**, 597 (2005).
- [28] A. Farjadpour *et al.*, Opt. Lett. **31**, 2972 (2006).
- [29] H. P. Urbach and S. F. Pereira, Phys. Rev. Lett. **100**, 123904 (2008).
- [30] U. Schröter and A. Dereux, Phys. Rev. B **64**, 125420 (2001).
- [31] S. Wedge and W. L. Barnes, Opt. Express **12**, 3673 (2004).
- [32] J. Renger, S. Grafström, and L. M. Eng, Phys. Rev. B **76**, 045431 (2007).